

# Top mass determination, Higgs inflation, and vacuum stability

Vincenzo Branchina<sup>1</sup>, Emanuele Messina<sup>2</sup>, Alessia Platania<sup>3</sup>

*Department of Physics and Astronomy, University of Catania, and INFN,  
Via Santa Sofia 64, I-95123 Catania, Italy*

## Abstract

The possibility that new physics beyond the Standard Model (SM) appears only at the Planck scale  $M_P$  is often considered. However, it is usually argued that new physics interactions at  $M_P$  do not affect the SM stability phase diagram, so the latter is obtained neglecting these terms. According to this diagram, for the current experimental values of the top and Higgs masses, our universe lives in a metastable state (with very long lifetime), near the edge of stability. Contrary to these expectations, however, we show that the stability phase diagram strongly depends on new physics and that, despite claims to the contrary, a more precise determination of the top (as well as of the Higgs) mass will not allow to discriminate between stability, metastability or criticality of the electroweak vacuum. At the same time, we show that the conditions needed for the realization of Higgs inflation scenarios (all obtained neglecting new physics) are too sensitive to the presence of new interactions at  $M_P$ . Therefore, Higgs inflation scenarios require very severe fine tunings that cast serious doubts on these models.

---

<sup>1</sup>branchina@ct.infn.it

<sup>2</sup>emanuele.messina@ct.infn.it

<sup>3</sup>a.platania90@gmail.com

# 1 Introduction

The discovery of the Higgs boson [1, 2] is certainly one of the most important findings of the last years, the experimental data are consistent with Standard Model (SM) predictions, and no sign of new physics has been detected. These results have boosted new interest and work on earlier speculations [3–20] that consider the possibility for new physics to show up only at very high energies, and for the electroweak vacuum to be unstable/metastable. A largely explored scenario assumes that new physics interactions only appear at the Planck scale  $M_P$  [20–25].

To study this scenario, the knowledge of the Higgs effective potential  $V_{eff}(\phi)$  up to very high values of  $\phi$  is needed. Due to top loop corrections,  $V_{eff}(\phi)$  bends down for values of  $\phi$  much larger than  $v$ , the location of the electroweak (EW) minimum, and develops a new minimum at  $\phi_{min} \gg v$ . Depending on Standard Model (SM) parameters, in particular on the top and Higgs masses,  $M_t$  and  $M_H$ , the second minimum can be higher or lower than the EW one. In the first case, the EW vacuum is stable. In the second one, it is metastable and we have to consider the lifetime  $\tau$  of the false EW vacuum and compare it with the age of the universe  $T_U$ . If  $\tau$  turns out to be larger than  $T_U$ , even though the EW vacuum is not the absolute minimum of  $V_{eff}(\phi)$ , our universe may well be sitting on such a metastable (false) vacuum. This is the so called metastability scenario.

This stability analysis is usually presented with the help of a stability phase diagram in the  $M_H - M_t$  plane (although, strictly speaking, this is not a phase diagram, following the common usage we continue to use this expression). The standard results [20–25] provide the plot shown in fig.1. The plane is divided into three different sectors. An *absolute stability* region (green), where  $V_{eff}(v) < V_{eff}(\phi_{min})$ , a *metastability* region (yellow), where  $V_{eff}(\phi_{min}) < V_{eff}(v)$ , but  $\tau > T_U$ , and an *instability* (red) region, where  $V_{eff}(\phi_{min}) < V_{eff}(v)$  and  $\tau < T_U$ . The stability line separates the stability and the metastability sectors, and is obtained for  $M_H$  and  $M_t$  such that  $V_{eff}(v) = V_{eff}(\phi_{min})$ . The instability line separates the metastability and the instability regions and is obtained for  $M_H$  and  $M_t$  such that  $\tau = T_U$ .

According to this analysis, given  $M_t \sim 173.34$  GeV (central value coming from the combination of Tevatron and LHC measurements [26]) and  $M_H \sim 125.7$  GeV (average value coming from the combination [27] of ATLAS and CMS results [28–31]), the experimental point (black dot of fig.1) lies inside the metastability region, and, within  $3\sigma$ , it could reach and even cross the stability line. When it sits on this line, a case named “critical”, the running quartic coupling  $\lambda$  and the beta function vanish at  $M_P$ ,  $\lambda(M_P) \sim 0$ , and  $\beta(\lambda(M_P)) \sim 0$ . From fig.1 we see that the black dot is close to the stability line, and the “near-criticality” of

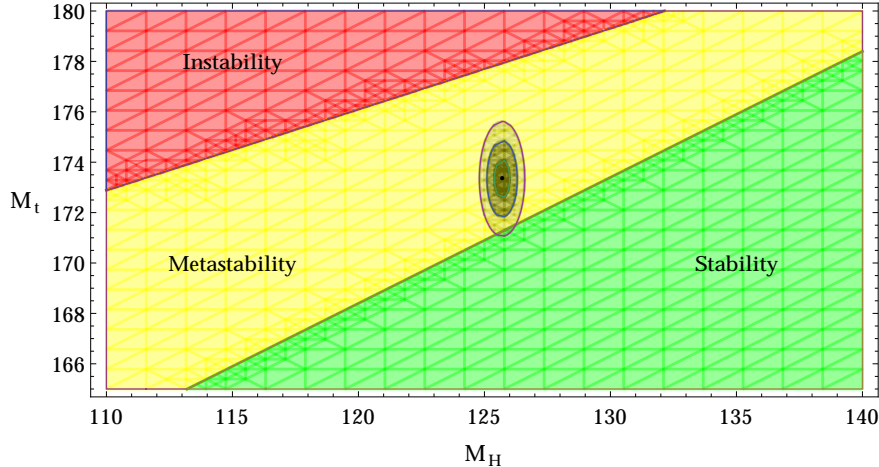


Figure 1: The stability phase diagram obtained according to the standard analysis. The  $M_H - M_t$  plane is divided in three sectors, stability (green), metastability (yellow), and instability (red) regions (see text). The dot is for  $M_H \sim 125.7$  GeV and  $M_t \sim 173.34$  GeV (current experimental values). The  $1\sigma$ ,  $2\sigma$  and  $3\sigma$  ellipses are also shown, the experimental uncertainties being  $\Delta M_H = \pm 0.3$  GeV and  $\Delta M_t = \pm 0.76$  GeV.

the experimental point is considered by some as the most important message from the data on the Higgs boson [25]. The Higgs inflation scenario of [32], in particular, strongly relies on the realization of the conditions  $\lambda(M_P) \sim 0$  and  $\beta(\lambda(M_P)) \sim 0$ .

Then, given this phase diagram, it is expected that, with the help of more refined measurements, we should be able to see whether the experimental point sits on the border between stability and metastability or is located inside one of these two regions. More precisely, as the dominant uncertainty comes from the value of the top mass, the expectation is that a more precise determination of  $M_t$  will finally allow to discriminate between a stable or metastable (or critical) EW vacuum [33], [34].

The above analysis, however, presents some delicate aspects. For the central values  $M_t \sim 173.34$  GeV and  $M_H \sim 125.7$  GeV, the Higgs potential  $V_{eff}(\phi)$  at  $M_P$  is negative (unstable),  $V_{eff}(\phi = M_P) < 0$ , and for  $\phi > M_P$  it continues to go down for a long while, developing the new minimum at  $\phi_{min}$  much larger than  $M_P$ ,  $\phi_{min} \sim 10^{30}$  GeV. Usually, this is not viewed as a serious drawback [20]. In fact, it is argued that  $V_{eff}(\phi)$  is eventually stabilized by new physics interactions present at the Planck scale, that should bring the new minimum around  $M_P$ . At the same time, it is also argued that the new physics terms should not affect the EW vacuum lifetime [20, 21], so the latter is computed by considering the unmodified potential  $V_{eff}(\phi)$ , i.e. neglecting the presence of new physics.

It has been recently shown, however, that the EW vacuum lifetime can be strongly

affected by new physics [35]. By carrying further on this analysis, in the present work we show that the expectation that better measurements of the top mass will allow to discriminate between a stable, a metastable or a critical EW vacuum [33,34] is not fulfilled. Even very precision measurements of the top mass  $M_t$  (as well as of  $M_H$ ) cannot decide of the EW vacuum stability condition. As we will see, the phase diagram of fig.1 can be strongly modified by the presence of new physics.

It is worth to stress, once again, that this phase diagram is obtained by requiring, on the one hand, that at the Planck scale new physics is present and should stabilize the Higgs potential (otherwise unstable) at this scale, and assuming, on the other hand, that these new physics interactions have no impact in determining the diagram itself. In the light of the results of the present work anticipated above, it is clear that this phase diagram should not any longer be used as the diagram to which we refer to decide of the stability condition of the EW vacuum. The main actor in determining whether the experimental  $(M_H, M_t)$  point lies in the stability or the metastability region is new physics, as the latter can strongly affect the stability phase diagram (the diagram of fig.1 can be radically changed).

At the same time, we show that when a specific UV completion of the SM, i.e. a specific BSM theory, is considered, the stability analysis that takes into account the new interactions provides a “stability test” for the BSM theory under investigation. In this framework, precision measurements of  $M_t$  (and/or  $M_H$ ) provide more stringent constraints in the parameter space of the theory.

The rest of the paper is organized as follows. In Section 2 we first review the usual analysis, by considering the case of absolute stability of the EW vacuum, and then we present the same analysis when new physics interactions are taken into account. In Section 3 we do the same for the metastability case. In particular, we show how the EW vacuum lifetime is computed in the presence of new physics. In Section 4, we present the new phase diagrams when a specific (toy model) form of new physics is taken into account. In this section we show how the presence of new physics interactions, far from being negligible, can strongly affect the stability phase diagram of the EW vacuum. In Section 5 we consider Higgs inflation scenarios and apply our analysis to these models, showing that the extreme sensitivity to new physics of the conditions that need to be realized in order for these models to be viable cast serious doubts on them. Section 6 is for our conclusions.

## 2 Stability analysis

We begin with a short review of the standard stability analysis [20–25], where new physics interactions at the Planck scale are neglected. Later, we present the corresponding analysis when new physics is taken into account.

The Higgs potential  $V_{eff}(\phi)$  bends down for values of  $\phi$  larger than  $v$  (location of the EW vacuum), and develops a new minimum at  $\phi_{min}$ . Depending on  $M_H$  and  $M_t$ , the latter can be lower, higher (or at the same height of) the EW minimum. Let us normalize  $V_{eff}(\phi)$  so that it vanishes at  $\phi = v$ . For large values of  $\phi$ ,  $V_{eff}(\phi)$  can be written as [13]

$$V_{eff}(\phi) \sim \frac{\lambda_{eff}(\phi)}{4} \phi^4, \quad (1)$$

where  $\lambda_{eff}(\phi)$  depends on  $\phi$  essentially as the running quartic coupling  $\lambda(\mu)$  depends on the running scale  $\mu$ .  $V_{eff}(\phi)$  is the renormalization group improved (RGI) Higgs potential, and for  $\lambda_{eff}(\phi)$  we have the corresponding one-loop, two-loops or three-loops expressions. In the following we consider the up to date Next-to-Next-to-Leading-Order (NNLO) results [24, 36–38].

For a large range of values of  $M_H$  and  $M_t$ ,  $\lambda_{eff}(\phi)$  has a minimum. Let us call  $\bar{\phi}_{M_H, M_t}$  the point where, for a given  $(M_H, M_t)$  couple,  $\lambda_{eff}(\phi)$  reaches this minimum. From Eq.(1), we see that the stability line in the  $(M_H, M_t)$ -plane (the line that separates the green and the yellow regions in fig.1) is obtained for those couples of values of  $M_H$  and  $M_t$  such that

$$\lambda_{eff}(\bar{\phi}_{M_H, M_t}) = 0, \quad (2)$$

as in this case  $V_{eff}(\phi_{min}) = V_{eff}(v)$ . The solid (blue) line of fig.2 provides an example, showing the running of  $\lambda_{eff}(\phi)$  for  $M_H = 125.7$  GeV and  $M_t \sim 171.43$  GeV (see the caption of the figure for an explanation of these values). The minimum of  $\lambda_{eff}(\phi)$  in this case is  $\bar{\phi}_{M_H, M_t} \sim 2.22 \cdot 10^{18}$  GeV.

We are now interested in studying what happens when new physics interactions at the Planck scale are taken into account. Following [35], we study the impact of new physics by adding to the potential two higher order operators,  $\phi^6$  and  $\phi^8$ . With the inclusion of these terms, the classical potential  $V(\phi) = \frac{\lambda}{4} \phi^4$  becomes ( $np$  is for new physics)

$$V_{np}(\phi) = \frac{\lambda}{4} \phi^4 + \frac{\lambda_6}{6} \frac{\phi^6}{M_P^2} + \frac{\lambda_8}{8} \frac{\phi^8}{M_P^4}, \quad (3)$$

with  $\lambda_6$  and  $\lambda_8$  dimensionless coupling constants.

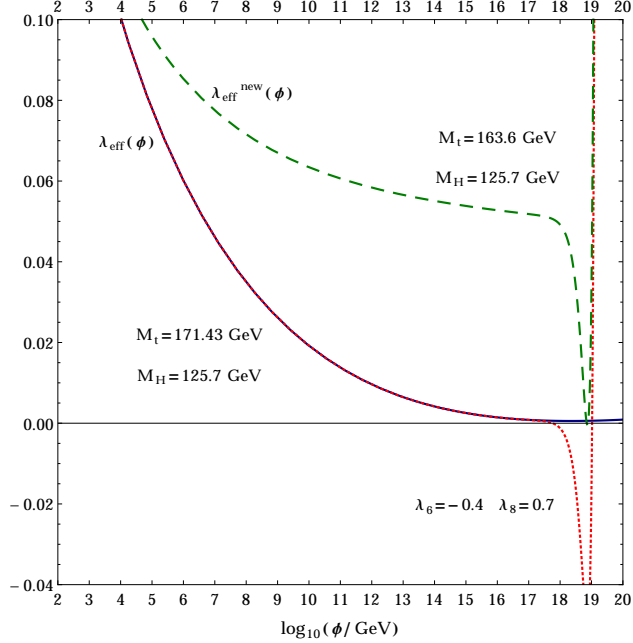


Figure 2: The solid (blue) line shows the running of  $\lambda_{eff}(\phi)$  for  $M_H = 125.7$  GeV and  $M_t$  adjusted so that  $\min_{\phi} \lambda_{eff}(\phi) = 0$  (see Eq.(2)). We get  $M_t \sim 171.43$  GeV, while the minimum is at  $\bar{\phi}_{M_H, M_t} \sim 2.22 \cdot 10^{18}$  GeV. The dotted (red) line shows the running of  $\lambda_{eff}^{new}(\phi)$  (Eq. (5)) for the same values of  $M_H$  and  $M_t$  and for  $\lambda_6 = -0.4$  and  $\lambda_8 = 0.7$ . The minimum is formed well below zero. Keeping fixed the values of  $M_H$ ,  $\lambda_6$  and  $\lambda_8$ , the dashed (green) line shows the running of  $\lambda_{eff}^{new}(\phi)$  for that value of  $M_t$  such that  $\min_{\phi} \lambda_{eff}^{new}(\phi) = 0$ . In this case, we get  $M_t = 163.3$  GeV.

Running the RG equations for all of the SM parameters, including  $\lambda_6$  and  $\lambda_8$ , we get the new RGI potential  $V_{eff}^{new}(\phi)$ ,

$$V_{eff}^{new}(\phi) = V_{eff}(\phi) + \frac{\lambda_6(\phi)}{6M_P^2} \xi(\phi)^6 \phi^6 + \frac{\lambda_8(\phi)}{8M_P^4} \xi(\phi)^8 \phi^8, \quad (4)$$

where  $\lambda_6(\phi)$  and  $\lambda_8(\phi)$ , as  $\lambda_{eff}(\phi)$ , are the RG improved couplings, and  $\xi(\phi)$  comes from the anomalous dimension of  $\phi$ . For the purposes of this work, however, it is sufficient to keep only the tree level corrections coming from the new operators, although the effect of the running can be easily taken into account.

The potential  $V_{eff}^{new}(\phi)$  modified by the presence of the new physics interactions is then obtained from Eq. (1), with  $\lambda_{eff}(\phi)$  replaced by

$$\lambda_{eff}^{new}(\phi) = \lambda_{eff}(\phi) + \frac{2}{3} \lambda_6 \frac{\phi^2}{M_P^2} + \frac{1}{2} \lambda_8 \frac{\phi^4}{M_P^4}, \quad (5)$$

and the stability line is given by those values of  $\phi$  such that (5) vanishes.

Let us consider natural (i.e.  $O(1)$ ) values for  $\lambda_6$  and  $\lambda_8$ , choosing, for instance,  $\lambda_6 = -0.4$  and  $\lambda_8 = 0.7$ . The dotted (red) line of fig.2 is obtained for these values of  $\lambda_6$  and  $\lambda_8$ .  $M_H$  and  $M_t$  are kept fixed to the same values used for the solid (blue) line ( $\lambda_6 = 0$ ,  $\lambda_8 = 0$ ). As expected, for  $\phi \ll M_P$ , the dependence on  $\phi$  of  $\lambda_{eff}^{new}(\phi)$  coincides with that of  $\lambda_{eff}(\phi)$ . Approaching  $M_P$ , however,  $\lambda_{eff}^{new}(\phi)$  becomes negative and develops a minimum well below zero.

If, for comparison, we again consider the case  $M_H = 125.7$  GeV, the corresponding value of  $M_t$  that brings the SM point (black dot of fig.1) on the stability line turns out to be sensibly different from the one previously determined in the absence of new physics. The dashed (green) line of fig.2 shows the running of  $\lambda_{eff}^{new}(\phi)$  for such a value of  $M_t$ . The latter now turns out to be  $M_t = 163.60$  GeV and has to be compared with the result obtained above in the absence of new physics,  $M_t = 171.43$  GeV.

In the present section we set up the tools for the determination of the stability line, with and without new physics interactions taken into account. In Section 4, where the stability phase diagrams are studied, we will make use of this analysis. In the next section, we move to the metastability case, i.e. we consider values of  $M_H$  and  $M_t$  such that the second minimum of  $V_{eff}(\phi)$  is lower than  $V_{eff}(v)$ . In these cases, the  $EW$  minimum is a false vacuum, and we need the tools to determine the instability line, i.e. the boarder between the region where the  $EW$  vacuum lifetime  $\tau$  is larger than the age of the universe  $T_U$ , and the region where  $\tau$  is shorter than  $T_U$ , the instability region.

### 3 EW vacuum lifetime. Metastability

The standard analysis of the metastability case is performed by computing the  $EW$  vacuum lifetime  $\tau$  with the help of the Higgs potential  $V_{eff}(\phi)$  that is obtained by considering SM interactions only [20–24]. As already noted in the Introduction, this is related to the expectation that new physics interactions should not affect  $\tau$ .

Referring to [20,23,24,35,39,40] for details, we recall here that for a given potential  $V(\phi)$ , the general procedure to obtain the tunnelling time  $\tau$  is to look first for the bounce solution (tree level) to the euclidean equation of motion [41], and to compute then the quantum fluctuations on the top of it [42]. For the Higgs potential  $V(\phi) = \lambda\phi^4/4$ , once the running of the quartic coupling is taken into account, this amounts to the following minimization formula

$$\tau = T_U \min_{\mu} \mathcal{T}(\mu) \tag{6}$$

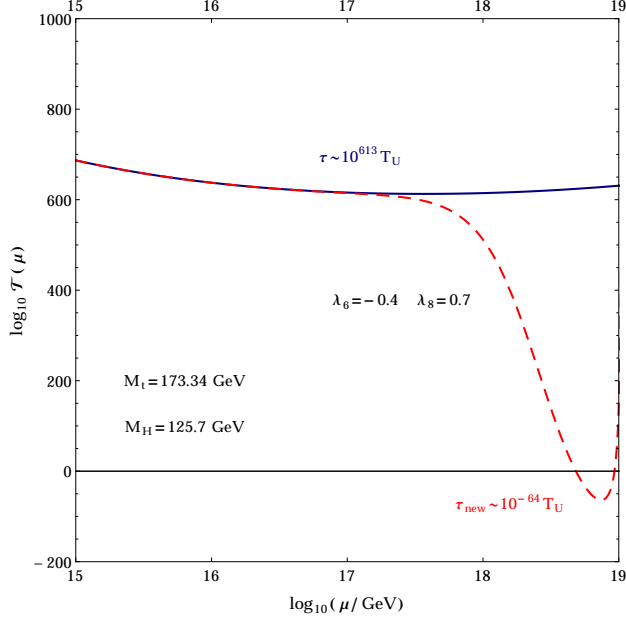


Figure 3: The solid (blue) line shows the function  $\log_{10} \mathcal{T}(\mu)$  for  $M_H = 125.7$  GeV and  $M_t = 173.34$  GeV (current experimental values). The minimum forms at  $\mu \sim 3.6 \cdot 10^{17}$  GeV, that gives  $\tau \sim 10^{613} T_U$ . The dashed (red) line shows  $\log_{10} \mathcal{T}_{new}(\mu)$  for the same values of  $M_H$  and  $M_t$  and for  $\lambda_6 = -0.4$  and  $\lambda_8 = 0.7$ . In this case the minimum is obtained for  $\mu \sim 0.62 M_P$ , that gives  $\tau_{new} \sim 10^{-64} T_U$ .

where  $\mathcal{T}(\mu)$  is

$$\mathcal{T}(\mu) \sim T_U^{-4} \mu^{-4} e^{\frac{8\pi^2}{3|\lambda_{eff}(\mu)|}}. \quad (7)$$

Together with Eq.(2), Eq.(6) is the other key ingredient of the standard stability analysis. The phase diagram of fig.1, in fact, is obtained with the help of these equations. The stability line (boarder between the stability and the metastability regions) in this figure is obtained for those values of  $M_H$  and  $M_t$  such that Eq.(2) is satisfied, the instability line (boarder between the metastability region,  $\tau > T_U$ , and the instability region,  $\tau < T_U$ ) for those values of  $M_H$  and  $M_t$  such that  $\tau = T_U$ .

From Eqs. (6) and (7), the condition  $\tau = T_U$  is immediately translated into the condition

$$\min_{\mu} \log_{10} \mathcal{T}(\mu) = 0. \quad (8)$$

The solid (blue) line of fig.3 is a plot of the function  $\log_{10} \mathcal{T}(\mu)$ , for  $M_H = 125.7$  GeV and  $M_t = 173.34$  GeV (central experimental values). This function has a minimum at  $\mu = \mu_{min} \simeq 3.6 \cdot 10^{17}$  GeV. The EW vacuum lifetime  $\tau$  turns out to be  $\tau \simeq 10^{613} T_U$ .

According to this analysis, then, for the central values  $M_H = 125.7$  GeV and  $M_t = 173.34$  GeV (black dot in fig.1), the EW vacuum is metastable and  $\tau$  is much greater than  $T_U$ . If we



now keep  $M_H$  fixed to the value  $M_H = 125.7$  GeV and increase  $M_t$ , we see that  $\tau$  decreases and reaches the value  $\tau = T_U$  for  $M_t = 178.04$  GeV. This is how the instability line is obtained.

As in the previous section, we want to perform now the stability analysis when the presence of new physics is taken into account. To this end, we consider again the potential  $V_{np}(\phi)$  of Eq.(3). We should then begin by considering the tree level contribution that comes from the new bounce solution for the potential (3). Differently from the previous case ( $\phi^4$  term alone), due to the presence of the terms  $\lambda_6\phi^6$  and  $\lambda_8\phi^8$ , this bounce cannot be found analytically, and we have to solve the Euclidean equation of motion numerically. Then, we should compute the quantum fluctuations around the bounce. This complete analysis is presented elsewhere [40].

Interestingly, in fact, a good approximate value of  $\tau$  can be obtained going back to Eqs.(6) and (7) and replacing in these equations  $\lambda_{eff}(\mu)$  with  $\lambda_{eff}^{new}(\mu)$  [35], where the latter is given in Eq.(5) (in [35]  $\lambda_{eff}^{new}$  is called  $\lambda_{eff}$ ). With this replacement, the tunnelling time is then given by [4, 9]

$$\tau_{new} = T_U \min_{\mu} \mathcal{T}_{new}(\mu), \quad (9)$$

where  $\mathcal{T}_{new}(\mu)$  is defined as  $\mathcal{T}_{new}(\mu) = T_U^{-4} \min_{\mu} (\mu^{-4} \exp(8\pi^2/(3|\lambda_{eff}^{new}(\mu)|)))$ .

We have carefully checked the validity of this approximation against the numerical computation of the bounce and of the corresponding quantum fluctuations [40] and found that the two results are in good agreement.

The dashed (red) line of fig.3 is a plot of the function  $\log_{10} \mathcal{T}_{new}(\mu)$  for  $\lambda_6 = -0.4$ ,  $\lambda_8 = 0.7$  and for the central experimental values of  $M_H$  and  $M_t$ . We note that, despite of the fact that  $\lambda_6$  and  $\lambda_8$  are natural ( $O(1)$  values), and we could expect that they would give negligible contribution to  $\tau$ , the impact of these new physics interactions on  $\tau$  is quite dramatic. The EW vacuum lifetime changes from  $\tau = 10^{613}T_U$  to  $\tau_{new} = 10^{-64}T_U$ .

As for the case of absolute stability considered in the previous section, from the example considered above we get the strong suggestion that new physics interactions at the Planck scale are far from being negligible. We come back to this point in the next section, where the phase diagrams are considered.

## 4 New physics, new phase diagrams and top mass

In the two previous Sections, we set up the tools for our analysis. We are now in the position to draw the stability phase diagram for different cases, with and without new physics interactions taken into account.

The phase diagram for the case when new physics interactions are neglected, as they are supposed to have no impact on it, is well known [24, 25], and we have reproduced this case in fig.1. From this figure we see that, according to this stability analysis, for the central values of  $M_H$  and  $M_t$ , the EW vacuum is metastable with a lifetime extremely larger than the age of the universe ( $\tau = 10^{613} T_U$ ). From the same diagram, we also see that, within  $3\sigma$ , the SM point could reach and even cross the stability line.

Due to the great sensitivity of the results on the stability analysis to the value of the top mass, it is usually believed that a more precise measurement of  $M_t$  would provide a definite answer to the question of whether we live in the stability region, in the metastability region, or at the edge of stability (criticality). In particular, it was stressed in [33] that the identification of the measured mass with the pole mass is not free of ambiguities (quarks do not appear as asymptotic states, and the pole top mass has to be defined with care), and that these difficulties can be overcome if we refer to the running  $M_t^{\overline{MS}}(\mu)$  top mass. At the same time, the authors observe that, when the translation to the pole mass is appropriately realized, the error on  $M_t$  turns out to be much larger than the experimental error usually reported. As a result, the Tevatron and LHC results for  $M_t$ , within two sigma, turn out to be consistent with stability, metastability, and instability at once. This analysis seems to point towards the conclusion that our knowledge of the stability condition of the EW vacuum critically depends on the precise determination of the top mass.

As we will see in a moment, however, while the remarks on the top pole mass [33] have to be seriously taken into account, the expectation that a more precise determination of the top mass will allow to discriminate between stability or metastability (or criticality) of the EW vacuum does not seem to be fulfilled. Even if new physics interactions show up only at the Planck scale, the “fate” of our universe (stability condition of the EW vacuum) crucially depends on this new physics.

This is clearly understood if now consider the phase diagram that we obtain by following the method presented in the two previous sections for a specific choice of new physics interactions. By taking the potential (3) as a model of new physics at the Planck scale  $M_P$ , choosing for instance  $\lambda_6 = -0.22$  and  $\lambda_8 = 0.4$ , we obtain the phase diagram of fig.4 (the

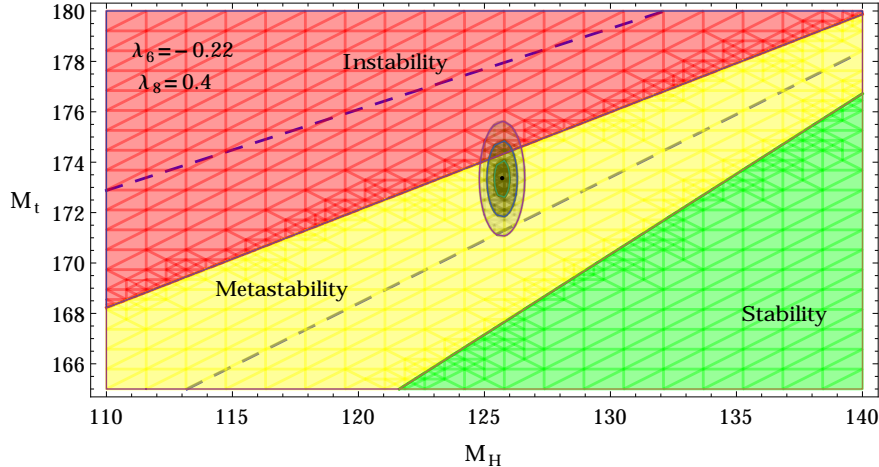


Figure 4: The stability phase diagram for the potential  $V(\phi) = \lambda\phi^4/4 + \lambda_6\phi^6/(6M_P^2) + \lambda_8\phi^8/(8M_P^4)$  with  $\lambda_6 = -0.22$  and  $\lambda_8 = 0.4$ . The  $M_H - M_t$  plane is divided in three sectors, stability, metastability, and instability regions. The dot indicates  $M_H \sim 125.7$  GeV and  $M_t \sim 173.34$  GeV. The  $1\sigma$ ,  $2\sigma$  and  $3\sigma$  ellipses are obtained for the experimental uncertainties  $\Delta M_H = \pm 0.3$  GeV and  $\Delta M_t = \pm 0.76$  GeV. The stability and instability lines of fig.1 (dashed lines) are reported for comparison.

dashed lines are for comparison and reproduce the phase diagram of fig.1). As a result of the presence of new physics at the Planck scale, the stability and metastability lines move down. For this choice of  $\lambda_6$  and  $\lambda_8$ , the SM point is still in the metastability region, but its distance from the stability line is larger than before (more than  $5\sigma$ ).

Comparing the stability phase diagram of fig.4 with the one of fig.1, we clearly see that even if the top mass is measured with very high precision, this is not going to give any definite indication on the stability condition of the EW vacuum. As long as we don't know the specific form of new physics, we cannot say anything on stability. Lowering the error in the determination of  $M_t$  is certainly important, but definitely not discriminating for the stability condition of the EW vacuum.

In order to better appreciate the strong dependence of the stability phase diagram on new physics, let us consider now a second example, where we use for  $\lambda_6$  and  $\lambda_8$  the values considered in Sections 2 and 3, namely  $\lambda_6 = -0.4$  and  $\lambda_8 = 0.7$ . It is important to note that (in this as in the previous example) we consider natural, i.e.  $O(1)$ , values for the new physics coupling constants. Therefore, the results that we get are not driven by an unnatural choice of large or small numbers for the (dimensionless) couplings. They can genuinely come from new physics beyond the SM.

The stability phase diagram for this new case is shown in fig.5. As compared to the

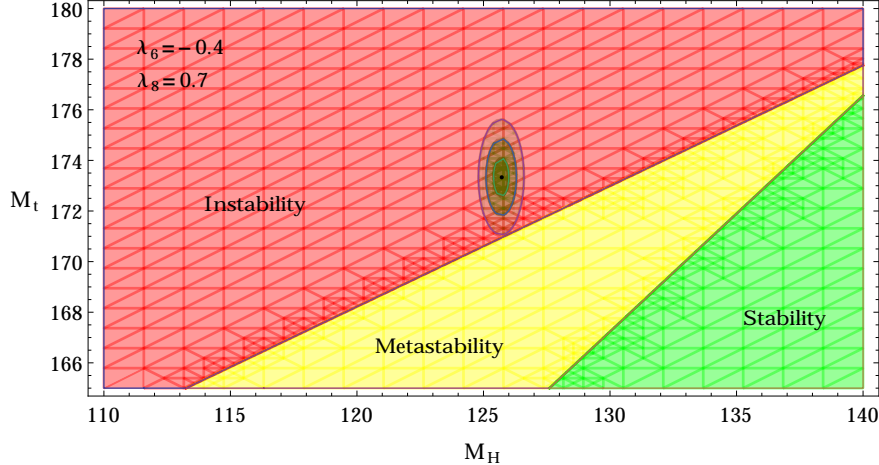


Figure 5: The stability phase diagram for the potential of fig.4 with  $\lambda_6 = -0.4$  and  $\lambda_8 = 0.7$ . The  $M_H - M_t$  plane is divided in three sectors, stability, metastability, and instability regions. The dot indicates  $M_H \sim 125.7$  GeV and  $M_t \sim 173.34$  GeV. The  $1\sigma$ ,  $2\sigma$  and  $3\sigma$  ellipses are obtained for the experimental uncertainties  $\Delta M_H = \pm 0.3$  GeV and  $\Delta M_t = \pm 0.76$  GeV.

previous case, the stability and metastability lines have moved even further down, so that, for the central experimental values of  $M_H$  and  $M_t$ , the SM point now lies in the instability region.

Figs. 4 and 5 clearly show that the stability phase diagram strongly depends on new physics. It is then clear that the diagram of fig.1 (that is the only case considered so far) is only one out of many different possibilities (see figs. 1, 4, 5). Whether the case of fig.1, or the case of fig.4, or another possible case is realized (of course the case of fig.5 is not possible for the simple reason that our universe has not decayed!) strongly depends on *which kind of new physics we have at the Planck scale*.

However, the phase diagram of fig.1 is usually presented as if it was the generic result that we obtain whenever we assume that the SM is valid all the way up to the Planck scale. In particular, referring to this phase diagram, it is stated that for the present experimental central values of  $M_H$  and  $M_t$ , our universe lives within the metastability region, at the edge of the stability line [25], and that better measurements of  $M_H$  and  $M_t$  will definitely allow to discriminate between stability, metastability or criticality for the EW vacuum [34].

In the light of what we have shown in the present work, these statements appear to be unjustified and misleading. What really discriminates between different stability conditions for the EW vacuum is *New Physics*. If new physics provides results of the kind that we have shown in fig.4, the phase diagram of fig.1 turns out to be simply wrong, and it has definitely nothing to say on the stability condition of the EW vacuum.

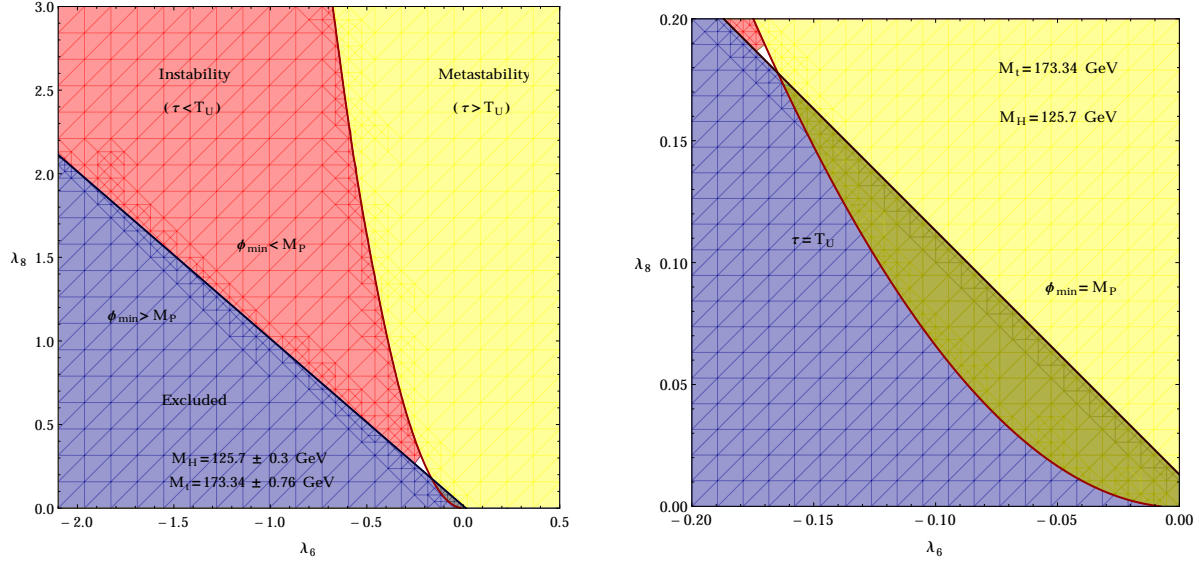


Figure 6: Left panel - The stability phase diagram in the  $(\lambda_6, \lambda_8)$  plane for the experimental values  $M_H = 125.7$  GeV and  $M_t = 173.34$  GeV. The instability (red) and metastability (yellow) regions are separated by the  $\tau = T_U$  line. The blue region is obtained for those values of  $\lambda_6$  and  $\lambda_8$  such that  $\phi_{min} > M_P$ , and the blue line separates the  $\phi_{min} > M_P$  and the  $\phi_{min} < M_P$  regions. Right panel - Magnification of the region in the lower part of the left panel diagram. For those values of  $\lambda_6$  and  $\lambda_8$  that lie in the dark green region,  $\tau$  is larger than  $T_U$  but the new minimum forms at  $\phi_{min} > M_P$ .

Therefore, it is incorrect and misleading to refer (as is usually done) to the phase diagram of fig.1 as to the diagram that provides the picture of the present situation for the SM assumed to be valid up to the Planck scale. We may well have the SM valid up to the Planck scale and, at the same time, a phase diagram as the one shown in fig.4. The stability phase diagram of fig.1, that is nothing but the well known and advertised diagram of [24, 25], is not universal, it is one case out of several different possibilities.

Let us move now to another important and related lesson that we can learn from the above results. Going back to the potential of Eq.(3), let us consider for  $M_H$  and  $M_t$  the current central experimental values,  $M_H = 125.7$  GeV and  $M_t = 173.34$  GeV, and draw the phase diagram of the SM in the  $(\lambda_6, \lambda_8)$  - plane. The usual analysis would tell us that, for these values of  $M_H$  and  $M_t$ , the EW vacuum is in the metastability region (see fig.1). We have seen, however, that the stability condition of the EW vacuum depends on new physics, i.e.  $\lambda_6$  and  $\lambda_8$  in our present case (see also [43]).

The left panel of fig.6 shows the vacuum stability phase diagram in the  $(\lambda_6, \lambda_8)$  - plane. The line separating the yellow and the red regions is the instability line ( $\tau = T_U$ ). The

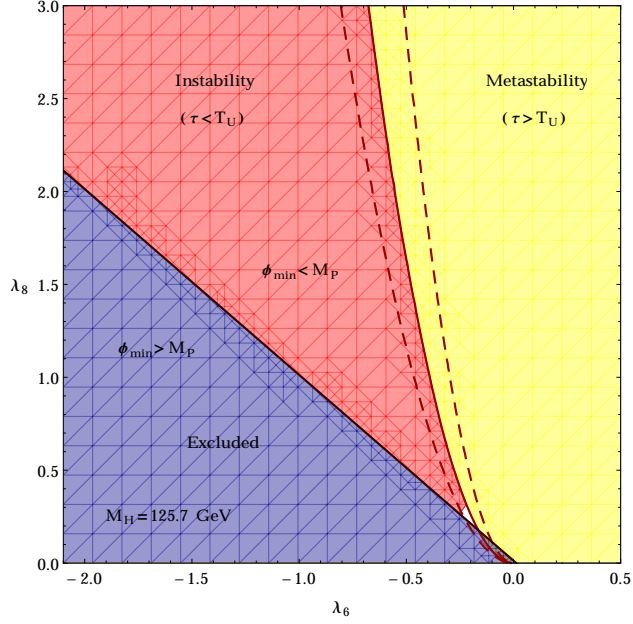


Figure 7: The same diagram as the left panel of fig.6, where  $M_H$  is kept fixed to the value  $M_H = 125.7$  GeV while for  $M_t$  a  $3\sigma$  excursion from the value  $M_t = 173.34$  GeV (dashed, red lines) is also considered. The experimental uncertainty is  $\Delta M_t = 0.76$  GeV.

metastability region ( $\tau > T_U$ ) is on the right side of this line, the instability region ( $\tau < T_U$ ) on the left. In this diagram we also see the appearance of a new boarder line, the line separating the red and the blue regions. For couples of values  $(\lambda_6, \lambda_8)$  in the blue region, the new minimum of the Higgs potential occurs at  $\phi_{min} > M_P$ , then we exclude this region of the parameter space. In this respect, we note that in the lower part of the diagram there is a region where  $\tau > T_U$  (then this region would be allowed from the point of view of the vacuum lifetime) but where  $\phi_{min} > M_P$ . The right panel of fig.6 shows a zoom on this region (dark green area).

The lesson from the above example is clear. Any beyond SM (BSM) candidate theory has to be tested with the help of a “stability test”. A BSM theory is acceptable only if it provides either a stable EW vacuum or a metastable one, but with lifetime larger than the age of the universe. A phase diagram of the kind shown in fig.6 allows to determine the regions of the parameter space that are permitted by the stability test.

At the same time, it is also clear that a more refined measurement of the top (as well as of the Higgs) mass provides more stringent constraints on the parameter space. Fig.7, for instance, shows the phase diagram in the  $(\lambda_6, \lambda_8)$  - plane, where  $M_H$  is kept fixed to the value  $M_H = 125.7$  GeV, as for fig.6, while for  $M_t$ , in addition to the central value  $M_t = 173.34$  GeV (solid line) of fig.6, we also consider  $3\sigma$  corrections to  $M_t$  (dashed lines), with  $\Delta M_t = 0.76$

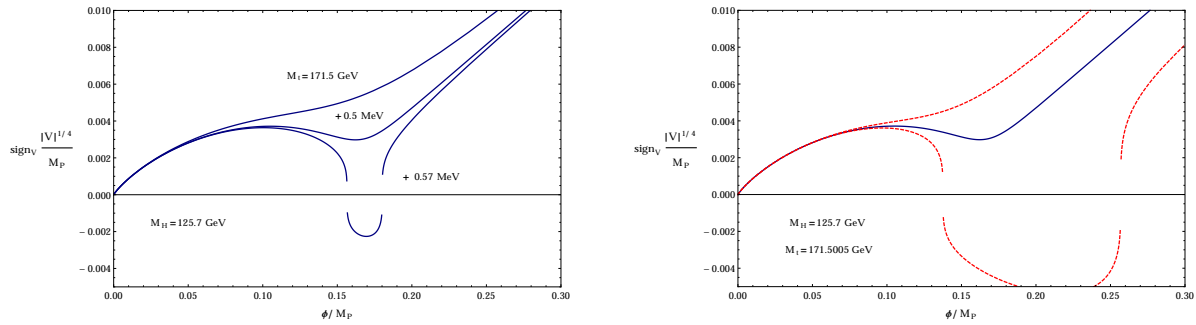


Figure 8: Left panel - From top to bottom : the *SM* Higgs Potential in  $M_P$  units for  $M_H = 125.7$  GeV and  $M_t = 171.5, 171.5005, 171.50057$  GeV. Right panel - The solid (blue) line is the *SM* Higgs Potential for  $M_H = 125.7$  GeV and  $M_t = 171.5005$  GeV. The dashed (red) upper line is the Higgs Potential in the presence of  $\phi^6$  and  $\phi^8$ , with  $\lambda_6 = 2.5 \cdot 10^{-4}$  and  $\lambda_8 = 1.6 \cdot 10^{-5}$ . The dashed (red) lower line gives the same Higgs potential for  $\lambda_6 = -1.17 \cdot 10^{-4}$  and  $\lambda_8 = 1.6 \cdot 10^{-5}$ .

GeV [26]. This is another important lesson of our analysis. While not discriminating for the stability issue, a better measurement of the top mass has an impact in the determination of the allowed regions in the parameter space of the theory.

## 5 Higgs Inflation and new physics

Let us come back now to the Higgs inflation scenario of [32]. As noted before, this scenario is heavily based on the standard vacuum stability analysis. In particular, it requires that new physics shows up only at the Planck scale  $M_P$ , and that the SM lives at the edge of the stability region, where  $\lambda(M_P) \sim 0$  and  $\beta(\lambda(M_P)) \sim 0$ . We have seen, however, that new physics interactions, even if they live at the Planck scale, can strongly change the SM phase diagram of fig.1. The realization of the conditions  $\lambda(M_P) \sim 0$  and  $\beta(\lambda(M_P)) \sim 0$  requires such a fine tuning [44] that even a small grain of new physics at the Planck scale can totally destroy the picture. We believe that these observation make the chance for the realization of the Higgs inflation scenario quite low.

Similar considerations also apply to an alternative implementation of Higgs inflation [45]. The idea is that we could have a second minimum that is higher than the EW one and such that this metastable state could have been the source of inflation in the early universe, later decaying in the EW stable minimum. In order to illustrate this scenario, together with our comments, we now consider the following case. Let  $M_H$  have the present central value,  $M_H = 125.7$  GeV, and consider values of  $M_t$  lower than the central value  $M_t = 173.34$  GeV,

actually values of  $M_t$  around  $M_t \sim 171.5$  GeV.

In the left panel of fig.8 we plot the Higgs effective potential computed with SM interactions only for  $M_t = 171.5, 171.5005, 171.50057$  GeV. We see that in the case  $M_t = 171.5005$  GeV the potential develops a new (shallow) minimum, higher than the EW one. As is clear from fig.8, there is only a narrow band of values of  $M_t$  such that this minimum is higher than the EW one. In fact (see fig.8), for  $M_t = 171.5$  GeV the minimum disappears, while for  $M_t = 171.50057$  GeV the new minimum is lower than the EW one.

Needless to say, this proposal has severe intrinsic fine tuning problems. Changing the fifth decimal in the top mass, the new minimum goes from metastable to stable. But even if we accept such a fine tuning for the top mass, and stick on the  $M_t = 171.5005$  GeV value of our example, the presence of even a little seed of new physics would be sufficient to screw up the whole picture. This is clearly shown in the right panel of fig.8, where the addition of very tiny values of new physics coupling constants is able to produce either the disappearance of the new minimum or the lowering of this minimum below the EW vacuum.

## 6 Conclusions

We have shown that the stability condition of the EW vacuum and the corresponding stability phase diagram in the  $(M_H, M_t)$  - plane strongly depend on new physics. On the contrary, in the past it was thought that, given the values of  $M_H$  and  $M_t$ , the stability of the EW vacuum could be studied with no reference to the specific UV completion of the SM. This led to the belief that the phase diagram of fig.1 is universal, that is independent on new physics. As we have shown, see figs.4 and 5, this is not the case.

This lack of universality has far reaching consequences for phenomenology, in particular for model building. As the stability condition of the EW vacuum is sensitive to new physics, it is clear that any BSM candidate has to pass a sort of “stability test”. In fact, only a BSM theory that respects the requirement that the EW vacuum is stable or metastable (but with lifetime larger than the age of the universe) can be accepted as a viable UV completion of the SM.

We have also shown that it is incorrect and misleading to refer to the phase diagram of fig.1 as if it was the snapshot of the present situation for a SM valid up to the Planck scale. As we have seen, *the SM may well be valid up to the Planck scale and still we could have a completely different stability phase diagram as compared to the phase diagram of fig.1*, the latter being the only one considered in the literature [24, 25]. This phase diagram is not



universal, it depends on the kind of new physics that we have at the Planck scale, it is just one case out of different possibilities. Therefore, we should no longer refer to this diagram as the status of art of our knowledge concerning the stability condition of the EW vacuum.

As a consequence of that, it is clear that, despite claims to the contrary, with a more precise determination of the top mass  $M_t$  we will not be able to discriminate between stability, metastability, or criticality of the EW vacuum. This expectation, in fact, is related to the (erroneous) assumption that the phase diagram of fig.1 is valid whatever new physics we have at the Planck scale.

At the same time, if we consider a specific UV completion of the SM (a specific BSM theory), a more precise knowledge of  $M_t$ , as well as of  $M_H$  and of the other parameters, will be important to put constraints on the parameter space of the theory. In other words, as long as we do not work with a specific BSM theory, we cannot draw any conclusions on the stability condition of the EW vacuum. Even if new physics shows up only at the Planck scale, the “fate” of our universe (that is the stability condition of the EW vacuum) crucially depends on the new physics interactions.

Moreover, it is clear that the same warnings apply to the Higgs inflation scenario of [32]. The latter is heavily based on the standard analysis, and in particular on the assumptions that new physics shows up only at the Planck scale  $M_P$  and that the EW vacuum is at the edge of the stability region, where  $\lambda(M_P) \sim 0$  and  $\beta(\lambda(M_P)) \sim 0$ . As we have seen, new physics interactions can strongly change the SM phase diagram of fig.1, thus changing these relations. In fact, the realization of the conditions  $\lambda(M_P) \sim 0$  and  $\beta(\lambda(M_P)) \sim 0$  requires an enormous fine tuning [44], and new physics interactions at the Planck scale can easily screw up these relations. Other implementations of the Higgs inflation idea [45], based on the possibility for the SM Higgs potential to develop a minimum at lower energies (a minimum where inflation could have started in a metastable state), are also subject, for the same reasons, to the same warnings.

Finally, it is important to note that our analysis on the impact of new physics interactions on the stability analysis can be repeated even when the new physics scale lies below the Planck scale, as could be the case, for instance, of GUT scale.

## References

- [1] ATLAS Collaboration, Phys. Lett. B710 (2012) 49.

- [2] CMS Collaboration, Phys. Lett. B710 (2012) 26.
- [3] N. Cabibbo, L. Maiani, G. Parisi, R. Petronzio, Nucl.Phys. B158 (1979) 295.
- [4] R. A. Flores, M. Sher, Phys. Rev. D27 (1983) 1679.
- [5] M. Lindner, Z. Phys. 31 (1986) 295.
- [6] D.L. Bennett, H.B. Nielsen and I. Picek, Phys. Lett. B 208 (1988) 275.
- [7] M. Sher, Phys. Rep. 179 (1989) 273.
- [8] M. Lindner, M. Sher, H. W. Zaglauer, Phys. Lett. B228 (1989) 139.
- [9] P. B. Arnold, Phys. Rev. D 40 (1989) 613.
- [10] G. Anderson, Phys. Lett. B243 (1990) 265.
- [11] P. Arnold and S. Vokos, Phys. Rev. D44 (1991) 3620.
- [12] C. Ford, D.R.T. Jones, P.W. Stephenson, M.B. Einhorn, Nucl.Phys. B395 (1993) 17.
- [13] M. Sher, Phys. Lett. B317 (1993) 159.
- [14] G. Altarelli, G. Isidori, Phys. Lett. B337 (1994) 141.
- [15] J.A. Casas, J.R. Espinosa, M. Quirós, Phys. Lett. B342. (1995) 171.
- [16] J.R. Espinosa, M. Quirós, Phys.Lett. B353 (1995) 257.
- [17] J.A. Casas, J.R. Espinosa, M. Quirós, Phys. Lett. B382. (1996) 374.
- [18] C. D. Froggatt and H. B. Nielsen, Phys. Lett. B 368 (1996) 96.
- [19] C.D. Froggatt, H. B. Nielsen, Y. Takanishi, Phys.Rev. D64 (2001) 113014.
- [20] G. Isidori, G. Ridolfi, A. Strumia, Nucl. Phys. B609 (2001) 387.
- [21] J. R. Espinosa, G. F. Giudice and A. Riotto, JCAP 0805 (2008) 002.
- [22] J. Ellis, J. R. Espinosa, G. F. Giudice, A. Hoecker and A. Riotto, Phys. Lett. B 679 (2009) 369.
- [23] J. Elias-Miro, J.R. Espinosa, G.F. Giudice, G. Isidori, A. Riotto, A. Strumia, Phys. Lett. B709 (2012) 222.

- [24] G. Degrassi, S. Di Vita, J. Elias-Miro, J. R. Espinosa, G. F. Giudice, G. Isidori, A. Strumia, JHEP 1208 (2012) 098.
- [25] D. Buttazzo, G. Degrassi, P. P. Giardino, G. F. Giudice, F. Sala, A. Salvio, A. Strumia, JHEP 1312 (2013) 089.
- [26] The ATLAS, CMS, D0 Collaborations, [arXiv:1403.4427](#) [hep-ex].
- [27] P. P. Giardino, K. Kannike, I. Masina, M. Raidal and A. Strumia, JHEP 1405 (2014) 046.
- [28] G. Aad et al. (ATLAS Collaboration), Phys.Lett. B726 (2013) 88.
- [29] S. Chatrchyan et al. (CMS Collaboration), [arXiv:1312.5353](#) [hep-ex].
- [30] Measurements of the properties of the Higgs-like boson in the two photon decay channel with the ATLAS detector using 25  $fb^1$  of proton-proton collision data, Tech. Rep. ATLAS-CONF-2013-012 (CERN, Geneva, 2013).
- [31] Updated measurements of the Higgs boson at 125 GeV in the two photon decay channel, Tech. Rep. CMS-PAS-HIG-13-001 (CERN, Geneva, 2013).
- [32] F.L. Bezrukov, M. Shaposhnikov, Phys.Lett. B659 (2008) 703; JHEP 0907 (2009) 089; F.L. Bezrukov, A. Magnin, M. Shaposhnikov, Phys.Lett. B675 (2009) 88.
- [33] S. Alekhin, A. Djouadi and S. Moch, Phys. Lett. B 716 (2012) 214.
- [34] G. Degrassi, [arXiv:1405.6852](#) [hep-ph].
- [35] V. Branchina, E. Messina, Phys.Rev.Lett. 111 (2013) 241801.
- [36] L.N. Mihaila, J. Salomon and M. Steinhauser, Phys. Rev. Lett. 108 (2012) 151602.
- [37] K. Chetyrkin and M. Zoller, JHEP 06 (2012) 033.
- [38] F. Bezrukov, M. Yu. Kalmykov, B. A. Kniehl, M. Shaposhnikov, JHEP 1210 (2012) 140.
- [39] V. Branchina, [arXiv:1405.7864](#) [hep-ph].
- [40] V.Branchina, E. Messina, in preparation.
- [41] S. Coleman, Phys. Rev. D15 (1977) 2929.

- [42] C. G. Callan, S. Coleman, Phys. Rev. D16 (1977) 1762.
- [43] Z. Lalak, M. Lewicki, P. Olszewski, JHEP 05 (2014) 119.
- [44] F. Bezrukov and M. Shaposhnikov, [arXiv:1403.6078](#) [hep-ph].
- [45] I. Masina, A. Notari, Phys.Rev. D85, 123506 (2012); I. Masina, [arXiv:1403.5244](#) [astro-ph.Co].